Molecular Human Reproduction, Vol.21, No.3 pp. 244–254, 2015
Advanced Access publication on December 1, 2014 doi:10.1093/molehr/gau110

molecular human reproduction

ORIGINAL RESEARCH

Kinetics of human sperm acrosomal exocytosis

C.M. Sosa[1,†], M.A. Pavarotti[1,†], M.N. Zanetti[1,2], F.C.M. Zoppino[1,3], G.A. De Blas[1,‡], and L.S. Mayorga[1,‡*]

[1]IHEM (CONICET-UNCuyo), School of Medicine, National University of Cuyo, 5500 Mendoza, Argentina
[2]Present address: Department of Cell Biology, Yale University School of Medicine, New Haven, CT, USA
[3]Present address: Laboratory of Oncology, Institute of Experimental Medicine and Biology of Cuyo (IMBECU – CONICET), 5500 Mendoza, Argentina

*Correspondence address. Casilla Correo 56, 5500 Mendoza, Argentina. Tel: +54-261-4494143 ext: 7001; Fax: +54-261-4494117 ext: 7050; E-mail: lmayorga@fcm.uncu.edu.ar

Submitted on July 18, 2014; resubmitted on October 15, 2014; accepted on November 23, 2014

ABSTRACT: The acrosome reaction is a unique event in the lifespan of sperm characterized by the exocytosis of the acrosomal content and the release of hybrid vesicles formed by patches of the outer acrosomal membrane and the plasma membrane. This unique regulated exocytosis is mediated by essentially the same membrane fusion machinery present in neuroendocrine cells. However, whereas secretion in neuroendocrine cells occurs in less than a second, the acrosome reaction is normally assessed after several minutes of incubation with inducers. In this report, we measured the kinetics of human sperm exocytosis triggered by two stimuli (calcium ionophore and progesterone) by using electron microscopy and three different approaches based on the incorporation of fluorescent Pisum sativum agglutinin into the acrosome upon opening of fusion pores connecting the extracellular medium with the acrosomal lumen. The results with the different methods are consistent with a slow kinetics ($t_{\frac{1}{2}} = 14$ min). We also manipulated the system to measure different steps of the process. We observed that cytosolic calcium increased with a relatively fast kinetics ($t_{\frac{1}{2}} = 0.1$ min). In contrast, the swelling of the acrosomal granule that precedes exocytosis was a slow process ($t_{\frac{1}{2}} = 13$ min). When swelling was completed, the fusion pore opening was fast ($t_{\frac{1}{2}} = 0.2$ min). The results indicate that acrosomal swelling is the slowest step and it determines the kinetics of the acrosome reaction. After the swelling is completed, the efflux of calcium from intracellular stores triggers fusion pores opening and the release of hybrid vesicles in seconds.

Key words: acrosomal swelling / acrosome reaction / fusion pore / regulated exocytosis / secretion kinetics

Introduction

The acrosome reaction is a regulated secretion with special characteristics that plays a central role in the fertilization process in many species. In particular, human spermatozoa possess a large flat granule covering the anterior part of the nucleus (Yanagimachi, 1994). The outer acrosomal membrane is in close proximity with the plasma membrane; however, these two membranes do not interact until the sperm is stimulated in the proximity of the mature oocyte to undergo the acrosome reaction. The stimulus induces a complex signal cascade that triggers an increase of calcium in the cytosol. The calcium signal is also complex, and presents several components, including an initial transient increase that is often followed by a sustained increase (Costello *et al.*, 2009; Darszon *et al.*, 2011). Acrosomal exocytosis involves the opening of a large number of fusion pores that expand in a particular manner leading to the release of hybrid vesicles. Probably the most crucial role for the acrosomal exocytosis is the change in the topology and composition of the limiting membrane of the sperm (Inoue *et al.*, 2011). The loss of the outer acrosomal and a large region of the plasma membrane exposes the inner acrosomal membrane to the medium and changes the composition of the plasma membrane, especially at the equatorial region. These changes are fundamental for the interaction and fusion of the sperm with the oocyte (Yanagimachi, 1994).

According to this description, acrosomal exocytosis seems to be different from other exocytic processes occurring in neuroendocrine cells both in topology and kinetics. In neurons, small secretory vesicles attached to specialized regions of the plasma membrane undergo fast secretion milliseconds after a cytosolic calcium increase (Jahn and Fasshauer, 2012; Sudhof, 2013). However, results from several laboratories, including ours, indicate that the membrane fusion machinery involved in the opening of fusion pores in neuroendocrine cells and in sperm share several components, including neurotoxin sensitive

[†] These authors contributed equally to the paper.
[‡] These authors share senior authorship.

SNARE proteins (Ward *et al.*, 1999; Michaut *et al.*, 2000; Ramalho-Santos *et al.*, 2000; Tomes *et al.*, 2002), SNARE complex interacting proteins [such as NSF (Zarelli *et al.*, 2009), αSNAP (Tomes *et al.*, 2005; Batiz *et al.*, 2009), complexin (Roggero *et al.*, 2007), synaptotagmin (Michaut *et al.*, 2001; Hutt *et al.*, 2002, 2005), Munc18 (Rodriguez *et al.*, 2012), Munc13 (Bello *et al.*, 2012)], Rab3 (Yunes *et al.*, 2000) and Rab3 interacting proteins [such as RIM (Bello *et al.*, 2012)].

The acrosome reaction is not a fast process. Results from several laboratories have shown that the percentage of reacted sperm increases with the time of incubation in the presence of physiological and pharmacological stimuli (Brewis *et al.*, 1996; Henkel *et al.*, 1998; Rockwell and Storey, 2000; Caballero-Campo *et al.*, 2006; Harper *et al.*, 2006, 2008). The kinetics of the process is measured in minutes and depending on the experimental conditions, it may require about 1 h to reach a plateau.

In this report, we measured the kinetics of human sperm exocytosis using four different approaches and two stimuli, a calcium ionophore and progesterone. We also manipulated the system to measure the kinetics of acrosomal swelling and fusion pore opening after the swelling was completed. The results indicate that swelling is the slowest process and it determines the kinetics of the acrosome reaction. After the swelling is completed, secretion occurs in seconds.

Materials and Methods

Reagents

A23187 was from Alomone Labs (Jerusalem, Israel). Progesterone, fluorescein isothiocyanate conjugated with Pisum sativum agglutinin (FITC-PSA), poly-L-lysine, and bovine serum albumin (BSA) were from Sigma-Aldrich Argentina SA. o-nitrophenyl-EGTA-acetoxymethyl ester (NP-EGTA AM), 1,2-bis-(o-aminophenoxy)ethane-N,N,N′,N′-tetraacetic acid-acetoxymethyl ester (BAPTA-AM), Fluo-3 AM and Fluo-5N AM were from Molecular Probes (Invitrogen Argentina). Xestospongin C and acetone were from Calbiochem (MERCK Química Argentina SAIC). All electron microscopy supplies were from Pelco (Ted Pella, Inc., CA, USA).

Sperm preparation

Human semen samples were provided by masturbation from healthy volunteer donors. The informed consent signed by the donors and the protocol for semen sample handling were approved by the Ethics Committee of the School of Medicine, National University of Cuyo. After sample liquefaction (20–30 min at 37°C), highly motile sperm were recovered by swim-up separation for 1 h in human tubal fluid media (HTF; as formulated by Irvine Scientific, Santa Ana, CA, USA) supplemented with 5 mg/ml BSA at 37°C in an atmosphere of 5% CO_2/95% air. Sperm suspensions were diluted to 10×10^6 sperm/ml with HTF-BSA and incubated 3–4 h to promote capacitation.

Acrosome reaction assays

Acrosome reaction (AR) was evaluated using the real-time, direct method and flow cytometry techniques described previously (Zoppino *et al.*, 2012). These methods are based on the incorporation of a fluorescent lectin (FITC-PSA) upon opening of fusion pores connecting the extracellular medium with the acrosomal lumen. The lectin prevents the diffusion of the acrosomal content after the vesiculation of the granule.

Real time

Capacitated sperm (5×10^6 cells/ml) were immobilized in poly-L-lysine (0.01% w/v) precoated coverslides. Samples were mounted in a chamber at 37°C and overlaid with HTF-BSA medium supplemented with 5 μg/ml FITC-PSA. The AR was induced with 10 μM ionophore (A23187) or 15 μM progesterone (Pg). Images were collected in an Olympus FV1000 confocal microscope or an Eclipse TE300 Nikon microscopy (2 frames/min). Image analysis was performed using the software Image J (National Institutes of Health, http://rsb.info.nih.gov/ij/). Background subtraction was performed using a region of interest placed as close as possible to the sperm of interest. Any incompletely adhered sperm that moved during the course of any experiment were discarded. Fluorescence measurements in individual sperm were made by manually drawing a region of interest around the head of each cell. When required, raw intensity values were expressed as relative fluorescence normalized to the maximum fluorescence obtained after the A23187 or Pg addition. The time of acrosome reaction initiation was recorded for each cell and a cumulative frequency was calculated (number of reacted sperm at time *t*/number of reacted sperm after 1 h *100).

Direct method and flow cytometry

Capacitated sperm (10×10^6 cells/ml) were incubated in HTF-BSA supplemented with 5 μg/ml FITC-PSA at 37°C and acrosome reaction induced by 10 μM A23187 or 15 μM Pg. At the end of the experiment, cells were fixed in 2% w/v paraformaldehyde in PBS for 10 min at room temperature. For direct method, the cells were then washed and resuspended at 10×10^6 cells/ml, spotted on slides, and air-dried. At least 200 cells were scored as 'reacted' (green acrosome) or 'not reacted' (not-stained acrosome) using a Nikon microscope equipped with epifluorescence optics. Negative (not stimulated) and positive (stimulated with 10 μM A23187 or 15 μM Pg) controls were included in all experiments. Ranges for reacted sperm after 15 min incubation: negative controls, 7–11%; A23187, 38–49%; Pg, 19–23%. For flow cytometry, fixed and washed cells were resuspended in PBS at 5×10^6 cells/ml. The preparation was analyzed (10 000 events) in a FACSAria flow cytometer (Becton Dickinson). The data were analyzed by FlowJo software. Negative (not stimulated) and positive (stimulated with 10 μM A23187) controls were included in all experiments. Ranges for reacted sperm after 60 min of incubation: negative controls, 5–21%; A23187, 41–84%; Pg 27–41%. Acrosomal exocytosis index was calculated by subtracting the number of reacted spermatozoa in the negative control from all values. The resulting values were expressed as a percentage of the AR observed in the positive control at the largest incubation time assayed in the particular experiment.

Transmission electron microscopy

Capacitated sperm (10×10^6 cells/ml) were incubated in HTF-BSA supplemented, when required, with 10 μM A23187 or 15 μM Pg and 5 μg/ml FITC-PSA. Samples were fixed in 2.5% v/v glutaraldehyde in PBS overnight at 4°C and prepared for electron microscopy as previously described (Zanetti and Mayorga, 2009). Ultrathin sections were observed and photographed under a Zeiss 902 electron microscope at 50 kV.

NP-EGTA AM assays

Capacitated sperm were incubated with 20 μM NP-EGTA AM at 37°C during 15 min in presence of FITC-PSA in the incubation medium. Acrosomal exocytosis was then initiated by adding 10 μM A23187 or 15 μM Pg during 15 min at 37°C. NP-EGTA AM was inactivated by UV light during 30 s. The reaction were stopped after 30, 60 and 120 s by fixation with 2% w/v paraformaldehyde in PBS for 10 min at room temperature (Direct Method and flow cytometry) or 2.5% v/v glutaraldehyde/PBS overnight at 4°C (Transmission Electron Microscopy). For real-time assays, the sperm were treated attached to the coverslips and the chelator inactivated under the microscope. Images were recorded at 2 frames/min during 15 min (before the UV flash) and at 1 frame/2.4 s during 2 min (after the flash).

$[Ca^{2+}]_i$ measurements

Capacitated sperm (10×10^6 cells/ml) were incubated with 2 μM Fluo-3 AM in the dark at 37°C during 30 min. Cells were washed once with HTF, immobilized on poly-L-lysine (0.01% w/v) precoated coverslips and mounted in a chamber at 37°C. Images were collected in an Olympus FV1000 confocal microscope (1 frame/2 s). The raw intensity values were normalized using the equations [(F/Fo)-1], where F is fluorescence intensity at time *t* and Fo is the mean of F taken during the control period. The resulting values were expressed as relative fluorescence normalized to the maximum fluorescence obtained after the A23187 or Pg addition.

Modeling with COPASI

A set of four differential equations were generated in the COmplex PAthway SImulator (COPASI) modelling program (http://www.copasi.org) (Hoops *et al.*, 2006), describing the 'capacitation', 'activation', 'swelling' and 'exocytosis' processes. Simple mass action for irreversible reactions was used for the kinetics of all reactions. The kinetics parameters introduced in the model were obtained from the $t_{\frac{1}{2}}$ in Fig. 4G ($ka = \ln 2 / t_{\frac{1}{2}}$). Experiments conducted with NP-EGTA AM were simulated introducing a condition where ka(exocytosis) was set to zero for times shorter than 'light/time' (an external parameter that can be changed for each simulation). Similarly, ka(capacitation) was set to zero unless A23187 was present and ka(activation) was set to zero unless A23187 or Pg were present. The ka(capacitation) refers to the changes induced by incubation with A23187 as reported by Tateno *et al.* (2013).

Results

Kinetics of acrosomal exocytosis

We have recently reported that FITC-PSA added to the incubation medium stains the acrosome of reacting sperm as it permeates into the secretory granule through the fusion pores connecting the extracellular medium with the acrosomal lumen (Zoppino *et al.*, 2012). The acrosomal matrix remains associated with the sperm head probably because the lectin cross-links and stabilizes this highly glycosylated structure. The method is suitable to follow acrosomal exocytosis in real time. When a population of cells attached to a coverslip was challenged with the calcium ionophore A23187, reacting sperm incorporated the fluorescent lectin. One striking observation was that not all sperm underwent exocytosis at the same time (Fig. 1A, blue circles). Sperm stimulated with ionophore, continued reacting for about 1 h after stimulation. Notice that all cells incorporated the fluorescent lectin with similar kinetics, suggesting that there were not major differences in the velocity of opening and expansion of the fusion pores. In contrast with the asynchrony of the acrosomal reaction, when the calcium entrance was imaged in sperm loaded with the Fluo-3 AM, most cells became fluorescent almost simultaneously upon addition of A23187 (Fig. 1A, light blue circles). When sperm were stimulated with progesterone (Fig. 1B, red squares), the acrosome reaction was also asynchronic, despite the fact that the rise in cytosolic calcium occurred in the first minute after stimulation (Fig. 1B). These observations indicate that initiation of the acrosomal exocytosis has a slow kinetics with a remarkable asynchrony that is not tightly coupled to the cytosolic calcium increase.

The cumulative frequency for sperm undergoing acrosome reaction at different times after A23187 stimulation was plotted in Fig. 2A. There was a striking difference in the kinetics between cytosolic calcium increase and acrosomal reaction. Most cells incorporated calcium in the first minute after A23187 addition (Supplementary Fig. S1) whereas acrosome reaction started in some sperm >30 min after stimulation (Fig. 2A and B, Supplementary Movie S1). The number of reacting cells that can be followed in real time is limited. Thus, we fixed the preparations at different times after stimulation and estimated the percentage of sperm with green acrosomes (reacted sperm) by regular fluorescence microscopy (Fig. 2C and D). With this static method, a similar kinetics of exocytosis was observed. The number of reacted sperm increased with time and a plateau was reached after about 1 h of incubation. To improve the estimation, similar experiments were performed and analyzed by flow cytometry. The population of reacted sperm was estimated counting 10 000 cells per condition. As shown in Fig. 2E and F, the number of reacted sperm increased with time, indicating that sperm that were intact at short times after challenging with the calcium ionophore, underwent exocytosis as the incubation continued.

The experiments were repeated using progesterone as a physiological inducer (Fig. 2A and 2B, Supplementary Movie S2, 2C, 2D and 2E). The percentage of sperm undergoing acrosome reaction was lower compared with the A23187 stimulus, independently of the method used to evaluate exocytosis. For example, reacted sperm ranged between 36 and 63% above the unstimulated control for $A23187_{60min}$, and between 12 and 28% for Pg_{60min} (evaluated by flow cytometry). However, the kinetics of the process was similar. The normalized percentages are shown in Fig. 2A (AR cumulative frequency), 2C

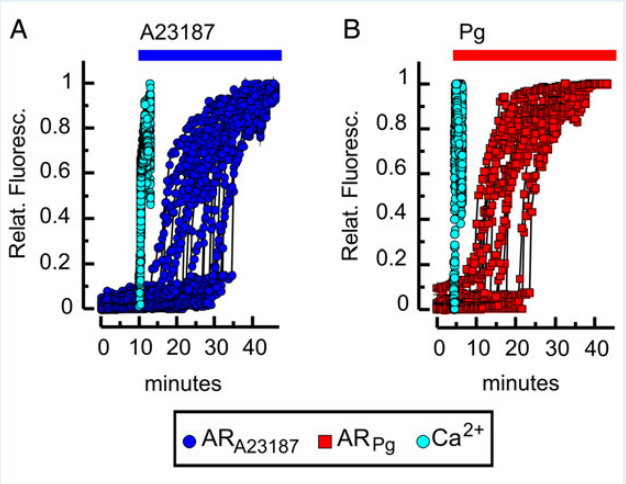

Figure 1 Kinetics of cytosolic calcium increase and acrosome reaction in real time. Cytosolic calcium increase and acrosomal exocytosis were followed in real time upon stimulation with 10 μM calcium ionophore (A23187) or 15 μM progesterone (Pg). To detect acrosomal exocytosis, capacitated human sperm were incubated in presence of fluorescein isothiocyanate conjugated with Pisum sativum agglutinin (FITC-PSA) in the incubation medium and then stimulated with A23187 (blue circles, left panel) and Pg (red squares, right panel). The cells were recorded at 2 frame/min during 60 min ($n = 400$ cells analyzed). To follow the increase of cytosolic calcium upon stimulation, capacitated human sperm were loaded with 2 μM Fluo-3 AM for 30 min at 37°C and the fluorescence intensity was measured before and after A23187 and Pg addition (light blue circles, **A** and **B**). Data were collected during 5 min at a frequency of 1 frame/2 s ($n = 20$ cells analyzed).

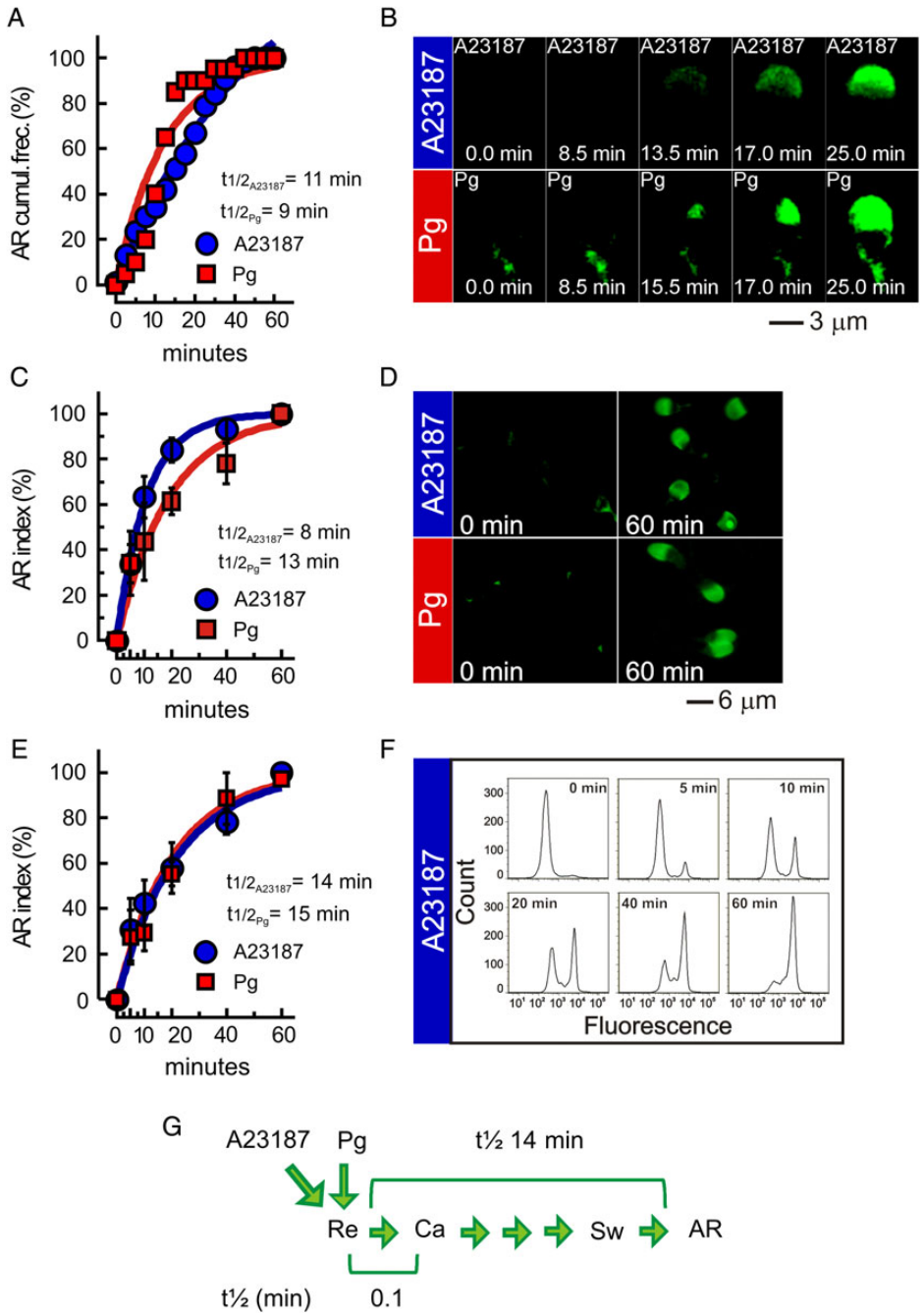

Figure 2 Acrosomal exocytosis in live cells recorded in real time and in fixed cell analyzed by fluorescent microscopy or by flow cytometry (FACSAria flow cytometer). Capacitated human sperm were incubated in presence of fluorescein isothiocyanate conjugated with Pisum sativum agglutinin (FITC-PSA) and the acrosome reaction was induced with 10 μM calcium ionophore (A23187) or 15 μM progesterone (Pg). Fluorescent lectin incorporation into the acrosome of live cells was monitoring at different times after stimulation under a confocal microscope (**A** and **B**), or in fixed cells by fluorescence microscopy (**C** and **D**) and flow cytometry (**E** and **F**). (A) Cumulative frequencies of 80 sperm undergoing acrosomal reaction at different times after stimulation with A23187 (blue circles) and Pg (red squares). (B) Representative FITC fluorescence changes in live cells after adding A23187 or Pg (top and bottom panel, respectively). (C) Acrosome reaction index at different times after stimulation with A23187 (blue circles) and Pg (red squares) measured by fluorescence microscopy in fixed cells. Values represent the mean ± SEM of three independent experiments. (D) Photomicrographs of FITC-labeled spermatozoa at 0 and 60 min after stimulation with A23187 or Pg (top and bottom panels, respectively). (E) Acrosome reaction index at different times after stimulation with A23187 (blue circles) and Pg (red squares) analyzed by flow cytometry in fixed cells. Values represent the mean ± SEM of three independent experiments. (F) Histograms of FITC-PSA fluorescence intensity at different times after stimulation with A23187. (**G**) A simplified scheme for acrosomal exocytosis represented by a sequence of reactions. The estimated $t_{\frac{1}{2}}$ for calcium entrance and global acrosome reaction are shown.

and 2E (AR index), red squares. In conclusion, physiological and pharmacological acrosome reaction inducers triggered exocytosis in responsive cells with a slow kinetics. All the experimental data were fitted to exponential curves, ideally corresponding to first order reactions. The kinetic constants from the fitting were transformed to half-time parameters ($t_{\frac{1}{2}}$; time to reach 50% of the maximum). The $t_{\frac{1}{2}}$ are shown in Fig. 2A, C and E. The estimation for the kinetics was in the 8–15 min range. This slow kinetics contrasts with the $t_{\frac{1}{2}}$ for sperm undergoing a calcium increase upon stimulation estimated in 0.1 min (Supplementary Fig. S1).

To perform a simplified analysis of the kinetics of the acrosome reaction, we represented this process in Fig. 2G. 'Re' stands for 'responsive cells' and 'AR' for 'acrosome reacted' cells and the arrows indicate known and unknown steps that lead to acrosomal exocytosis. Some steps were included in the model. Ca indicates the rise in cytosolic calcium that initiates acrosomal exocytosis. 'Sw' stands for the swelling and deformation of the acrosomal granule that promote the docking of the outer acrosomal and the plasma membranes before membrane fusion (Zoppino *et al.*, 2012). The triple arrows before Sw indicate that the mechanism connecting the calcium increase and swelling is not known. The estimated kinetics parameters were included in the model. For the global process, we chose the parameter that we considered more reliable (flow cytometry upon A23187 stimulation).

Kinetics of swelling

Acrosomal exocytosis requires dramatic changes in the topology of the fusing membranes. We have reported that swelling of the acrosome is part of the process by which the outer acrosomal membrane and the plasma membrane form tight appositions that are stabilized by the formation of trans SNARE complexes (Zanetti and Mayorga, 2009). We wondered whether the swelling in preparation for secretion could be a rate-limiting step for exocytosis. To analyze the kinetics of swelling after stimulation with A23187, exocytosis was blocked by adding an IP_3-dependent calcium channel inhibitor (xestospongin C). The rationale behind these experiments is that the ionophore affects mostly the plasma membrane causing a strong increase of cytosolic calcium but has a minor effect on the acrosomal membrane, preserving a functional acrosomal calcium store. Experiments performed to assess directly these assumptions validated the assay (Supplementary Fig. S2). We and many others have previously shown that the release of calcium from intracellular stores, presumably the acrosome, is necessary for the final membrane fusion step leading to acrosomal vesiculation (De Blas *et al.*, 2002, 2005; Herrick *et al.*, 2005). Inhibitors of IP_3-sensitive calcium channels do not block acrosomal swelling (Zanetti and Mayorga, 2009). Samples were fixed at different times after stimulation and the acrosome morphology evaluated by electron microscopy. The percentages of sperm with intact acrosomes, swollen acrosomes and no acrosomes (reacted sperm) as a function of time are shown in Fig. 3A. Micrographs in Fig. 3B represent examples of sperm with intact, swollen, vesiculated and lost acrosomes. The experimental data were fitted to exponential curves corresponding to first order reactions. The half-life of the process was in the order of 13 min, similar to the $t_{\frac{1}{2}}$ of the acrosome reaction (Fig. 2G), suggesting that swelling is a slow process that can strongly influence acrosomal exocytosis kinetics. We then added one more kinetics parameter to the model (Fig. 3C).

Kinetics of membrane fusion and acrosomal vesiculation

In neuroendocrine cells, the exocytosis of secretory granules attached to the plasma membrane is a fast event. However, the last step in the acrosome reaction is unique. It requires the opening and expansion of multiple fusion pores to release hybrid vesicles formed by patches of outer acrosomal and plasma membranes. We wondered whether the resolution of the exocytosis in sperm whose acrosomes were already swollen was a fast process. For these experiments, exocytosis was blocked loading the sperm with the photosensitive calcium chelator NP-EGTA AM (De Blas *et al.*, 2005). The incubation and concentration of the chelator was adjusted to allow the compound to accumulate in the acrosomal granule (Herrick *et al.*, 2005; Lopez *et al.*, 2007). We assumed that stimulation with A23187 would overcome the chelating capacity of the NP-EGTA AM retained in the cytoplasm, but would not be able to induce exocytosis because calcium in intracellular stores would be chelated. Experiments performed to assess directly these assumptions validated the assay (Supplementary Figs S3 and S4). We observed that sperm under these conditions underwent swelling but not exocytosis. Notice that the depletion of intracellular calcium stores is equivalent to preventing the release of calcium with the IP_3-sensitive calcium channel inhibitor used in the experiments in Fig. 3. The advantage here is that the inhibition is reversible. When the chelator was photoinactivated, the secretory process resumed. The kinetics of this step was followed in fixed cells counting the percentage of sperm with green acrosomes (reacted sperm) by fluorescence microscopy and flow cytometry (Fig. 4A and C, respectively). In striking contrast to what was observed without the calcium chelator, exocytosis was accomplished in seconds after photoinactivation of NP-EGTA AM (blue circles in Fig. 4A and C). This observation indicates that the opening and expansion of the fusion pores was not responsible for the slow kinetics of the acrosome reaction. A similar kinetics was observed when sperm were stimulated with progesterone (Fig. 4A, red squares).

In these experiments, to achieve fast exocytosis, sperm were stimulated with A23187 in the presence of NP-EGTA AM for 15 min. We then asked about the kinetics of acquisition of fast exocytosis. For these experiments, the sperm were loaded with NP-EGTA AM and swelling was induced by incubation with A23187 for different periods of time (0, 5, 10 and 15 min). NP-EGTA AM was then inactivated by UV light and sperm incubated for a short period of time (2 min) to induce exocytosis only in pre-activated sperm (Fig. 4B and D). Acrosomal exocytosis was evaluated by fluorescent microscopy (Fig. 4B) and by flow cytometry (Fig. 4D). Notice that the kinetics of acquiring fast exocytosis characteristics was similar to the kinetics of swelling shown in Fig. 3.

The NP-EGTA AM protocol was also used to follow exocytosis in real time. As shown in supplementary data (Supplementary Fig. S5), exocytosis started immediately after illumination, strikingly faster than when sperm were not preincubated under conditions that promote swelling. Notice that kinetics of incorporation of FITC-PSA were similar to those observed with the regular assay, suggesting that when exocytosis was initiated, the opening and expansion of fusion pores followed a similar kinetics under both conditions.

Finally, the NP-EGTA AM assay was followed by electron microscopy (Fig. 5). The sperm were stimulated for 15 min with A23187 in the presence of NP-EGTA AM and the samples fixed at short times after

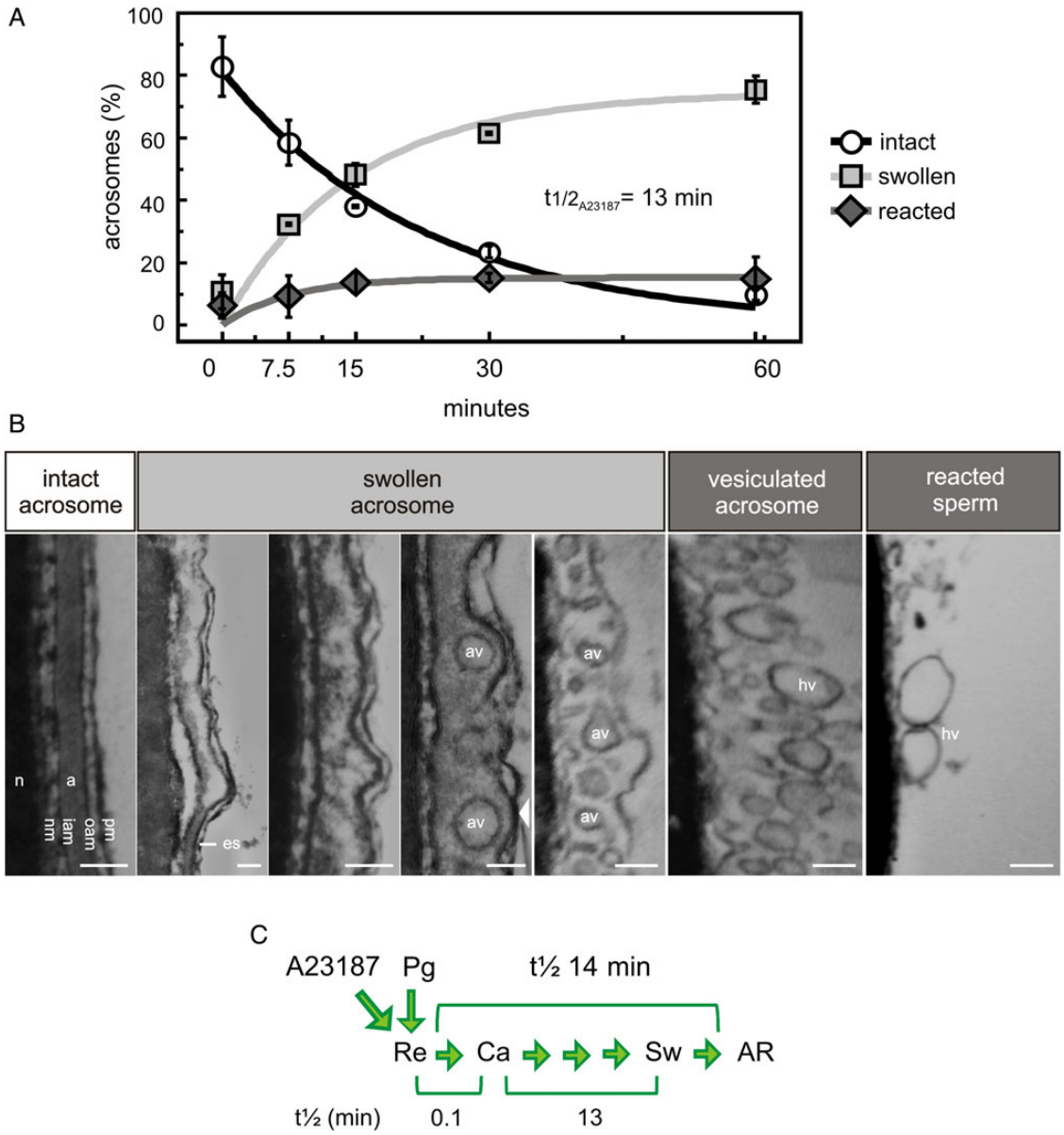

Figure 3 Kinetics of acrosomal swelling after stimulation with A23187. Capacitated sperm were stimulated with 10 μM of calcium ionophore (A23187) in the presence of 1 μM xestospongin C (to prevent acrosomal exocytosis). The reaction was stopped with 2.5% v/v glutaraldehyde and then processed for electron microscopy. (**A**) Percentage of sperm with intact acrosomes (white circles), swollen acrosomes (gray squares) or reacted sperm (dark gray rhomboids). The data represent the mean ± range of two experiments. Electronmicrographs in (**B**) illustrate different stages of acrosome reaction (intact, swollen, or vesiculated acrosome, and reacted sperm). a, acrosome; iam, inner acrosomal membrane; oam, outer acrosomal membrane; n, nucleus; nm, nuclear membrane; es, equatorial segment; av, intra acrosomal vesicle; hv, hybrid vesicle. Bars: 100 nm. (**C**) Simplified scheme for acrosomal exocytosis where the estimated $t_{\frac{1}{2}}$ for acrosomal swelling was included.

photoinactivation of the chelator. Observations of samples incubated with A23187 before NP-EGTA AM inactivation confirmed that these conditions promoted swelling (percentage of sperm with swollen acrosomes at zero time, Fig. 5A). After photoinactivation of the chelator, the percentage of sperm with vesiculated acrosomes increased rapidly. An important observation was that as the percentage of reacted sperm increased, the population of sperm with swollen acrosomes decreased, suggesting that these sperm were undergoing the acrosome reaction. The percentage of reacted sperm observed under these conditions after 2 min of incubation was similar to the one recorded in the same samples stimulated for 15 min with A23187 in the absence of NP-EGTA AM (Fig. 5A, bars). This indicates that the incubation with the photosensitive chelator was not affecting the percentage of sperm capable of undergoing acrosomal exocytosis. Electron microscopy images showing sperm in different stages of hybrid vesicle formation are shown in Fig. 5B. In conclusion, the results using the photosensitive

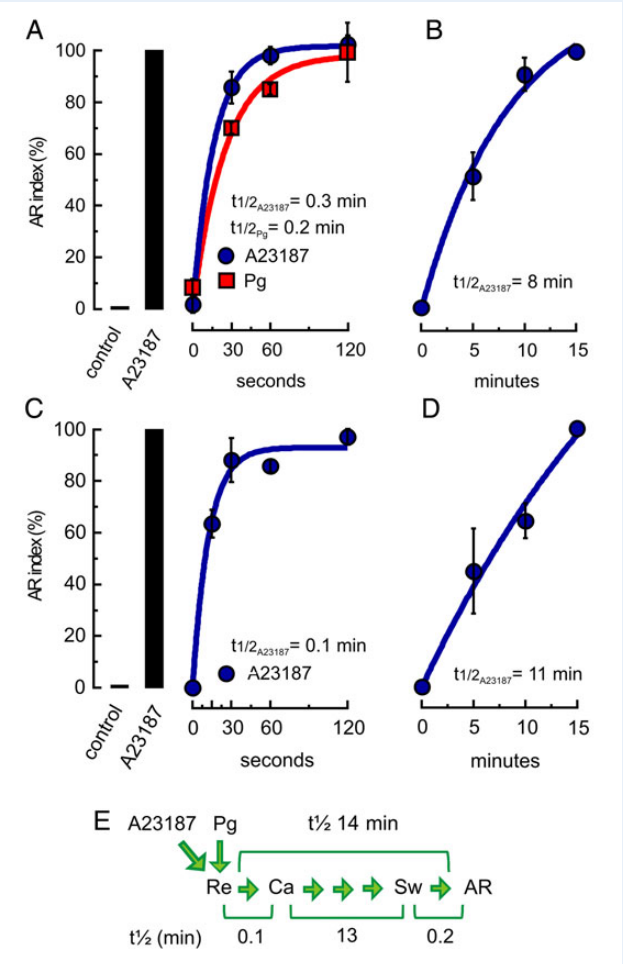

Figure 4 Kinetics of pore opening after acrosomal swelling. Capacitated human sperm were incubated for 15 min at 37°C in the presence of fluorescein isothiocyanate conjugated with Pisum sativum agglutinin (FITC-PSA) without stimulation (control, black bar; **A** and **C**) or in presence of 10 μM calcium ionophore (A23187, black bar; A and C). Some aliquots were loaded with 20 μM o-nitrophenyl-EGTA-acetoxymethyl ester (NP-EGTA AM) for 15 min at 37°C to chelate intra-acrosomal calcium. Acrosomal exocytosis was then initiated by adding 10 μM A23187 (blue circles, A and **B**) or 15 μM progesterone (Pg) (red squares, A). (A and C) After 15 min incubation at 37°C in the dark, the chelator was photoinactivated and the cells fixed at different time (0, 30, 60 and 120 s). The acrosome reaction was evaluated by fluorescence microscopy (A) or flow cytometry (C). (B and **D**) Sperm loaded with NP-EGTA AM were stimulated for 0, 5, 10 or 15 min with 10 μM A23187 in the presence of FITC-PSA in the dark. The chelator was photoinactivated and the cells were fixed 2 min after the flash. The acrosome reaction was evaluated by fluorescence microscopy (B) or flow cytometry (D). Values represent the mean ± SEM of three independent experiments. (**E**) Simplified scheme for acrosomal exocytosis where the estimated $t_{\frac{1}{2}}$ for fusion pore opening and expansion was included.

calcium chelator indicate that the opening and expansion of the fusion pores are relatively fast processes that are completed in a few seconds. This new kinetic parameter was then added to the model (Fig. 4E). In conclusion, the cytosolic calcium increase and the acrosome vesiculation steps are relatively fast processes, whereas acrosomal swelling has a slow kinetics with at $t_{\frac{1}{2}}$ similar to the one of the AR.

Discussion

Spermatozoa undergo many changes from the moment they are stimulated until exocytosis is completed. Initially, the secretory stimulus triggers a still not well-characterized signaling cascade leading to a calcium increase in the cytosol. This is a fast process. Seconds after progesterone or a calcium ionophore is applied, calcium signals are detected in real-time experiments (Harper *et al.*, 2003; Jimenez-Gonzalez *et al.*, 2006; Darszon *et al.*, 2011; Sanchez-Cardenas *et al.*, 2014). Calcium triggers a complex intracellular cascade of events leading to the swelling of the acrosome and docking of the acrosomal granule to the plasma membrane at the protruding edges of deep invaginations of the outer acrosomal membrane (Zanetti and Mayorga, 2009). Finally, fusion pores open, the acrosomal contents disperse and exocytosis is completed.

In this report, we have measured the apparent rate constant corresponding to the complete process from stimulation to acrosomal vesiculation using four different approaches to measure the onset of acrosomal exocytosis and two different stimuli, a calcium ionophore and progesterone. Not all assays rendered the same half-life for secretion; the values varied between 8 and 15 min. This range corresponds to a very slow exocytic event when compared with secretion in neuroendocrine cells. Other groups have assessed acrosomal exocytosis following the incorporation of fluorescent probes into the acrosome after stimulation with A23187 and progesterone. By using fluorescent soy bean trypsin inhibitor (SBTI), Harper and collaborators (Harper *et al.*, 2008) reported a mean latency after stimulation of ~15 min. Once exocytosis was initiated, the uptake of the probe followed a kinetics similar to those shown in Fig. 1A and B. SBTI does not stabilize the acrosomal matrix and was slowly lost as the acrosomal content dispersed. Sanchez-Cardenas and collaborators (Sanchez-Cardenas *et al.*, 2014) followed the incorporation of the membrane probe FM4-64 into acrosomal membranes as the fusion pores opened. They also reported a similar delay in acrosomal exocytosis. The probe permeated into the acrosomal membranes with a kinetics similar to those shown in Fig. 1A and B. Our results and those of these two laboratories using similar protocols but different probes show a remarkable asynchrony in the onset of exocytosis and a comparatively fast kinetics of incorporation of the probe into the acrosomes, suggesting that the opening and expansion of fusion pores occur in < 1 min.

One of the striking peculiarities of acrosomal exocytosis is the swelling and deformation of the acrosomal granule leading to the formation of deep invaginations of the outer acrosomal membrane. We set up conditions to measure the kinetics of the swelling and we found that the process also has slow kinetics. In contrast, when acrosomal swelling was completed, the last steps of the exocytosis, corresponding to the opening and expansion of the fusion pores to release hybrid vesicles, were comparatively fast. The kinetics of a concatenated process is determined by the slowest step. For acrosome reaction, the swelling of the acrosomal granule in preparation for membrane fusion is likely the rate-limiting step.

Although the kinetics of acrosomal reaction triggered by the calcium ionophore and progesterone were similar, the percentage of responsive cells was very different. Progesterone induced exocytosis in a small population of sperm, those that presumably had completed capacitation. The

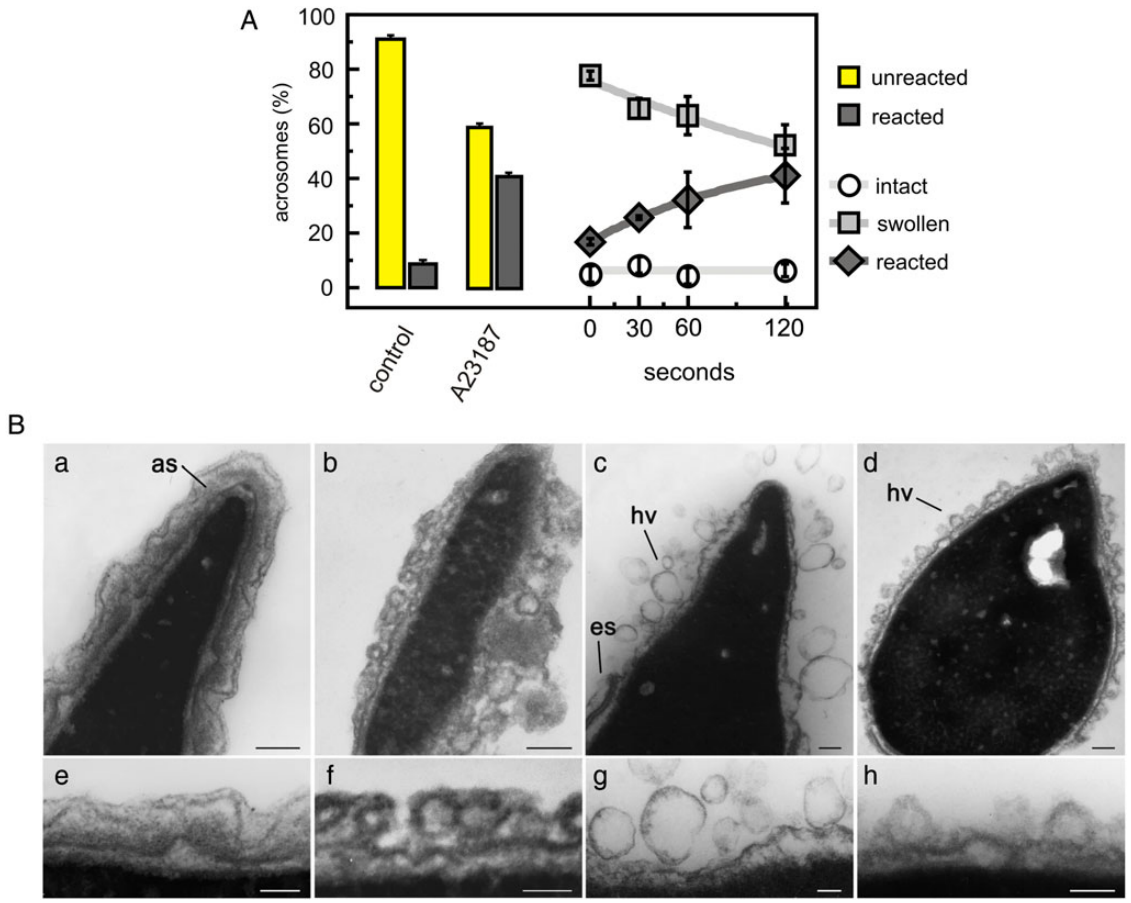

Figure 5 Kinetics of pore opening after acrosomal swelling monitored by electron microscopy. The time course of acrosome reaction in swollen sperms was evaluated by electron microscopy. (**A**) After capacitation, human sperm were incubated for 15 min at 37°C without any treatment (control) or treated with 10 μM calcium ionophore (A23187). The samples were fixed and processed for electron microscopy. The percentage of sperm with (unreacted, yellow bars) or without (reacted, gray bars) acrosome was estimated for each condition. In the same experiments, some aliquots were loaded with 20 μM o-nitrophenyl-EGTA-acetoxymethyl ester (NP-EGTA AM) for 15 min at 37°C to chelate intra-acrosomal calcium. Acrosomal exocytosis was initiated by adding 10 μM A23187. After 15 min incubation at 37°C in the dark, the chelator was photoinactivated and the samples were fixed in 2.5% v/v glutaraldehyde at short times after the UV flash (0, 30, 60 and 120 s). The samples were processed for electron microscopy and the percentage of sperm with intact acrosomes (white circles), swollen (light gray squares), and without acrosome (dark gray rhomboids) were estimated. The data represent the mean ± range of two experiments. (**B**) Electronmicrographs in a–h illustrate different stages of the acrosome after inactivation of the calcium chelator. a, sperm with a swollen acrosome; b, sperm in the first steps of vesiculation; c, sperm with a vesiculated acrosome; d, sperm that has completed the acrosome reaction (as, acrosome swelling; n, nucleus; es, equatorial segment; hv, hybrid vesicle). e, to h, higher magnification of a to d images showing details of the exocytic process. Bars, 500 nm (a–d) and 100 nm (e–h).

calcium ionophore, in contrast, triggered secretion in a larger proportion of sperm. The requirement to respond to A23187 may be different and independent of capacitation or, alternatively, the high concentrations of calcium in the cytosol may rapidly change the sperm to a responsive state. Recently, it was shown that 10 min incubation with A23187 makes mouse sperm capable of fertilizing mature oocytes (Tateno *et al.*, 2013). If sperm acquire exocytotic capability in the presence of the ionophore at a comparatively fast speed, the overall kinetics of the process would be similar, but the percentage of responding cells, larger.

With the aim of reproducing the experimental data by using a simple model with the kinetics parameters estimated in this report, the reactions shown in Fig. 6D were modeled in COPASI (ww.copasi.org) (Hoops *et al.*, 2006). The reactions are listed in Fig. 6D, and the kinetic constants for first order mass action reactions taken form the half time shown in Fig. 4E. Speculating that A23187 switches sperm from an 'unresponsive' to a 'responsive' state with a $t_{\frac{1}{2}}$ of ~1 min, the model can reproduce the results shown in Fig. 2A, C and E, for both, A23187 and progesterone stimuli (Fig. 6A). Adding an inhibitor that blocks the Sw → AR reaction, the model reproduces the results in Fig. 3 (compare Fig. 3A with Fig. 6B). Moreover, by programing a reversible inhibition of this reaction, the model is consistent with the results obtained with NP-EGTA AM observations shown in Fig. 4 (Fig. 6C, enlarged at the right). Based on the results, a model for acrosomal exocytosis steps and their kinetics is presented in Fig. 7.

The kinetics of human sperm acrosome reaction have been measured by several groups using different experimental approaches (Brewis *et al.*,

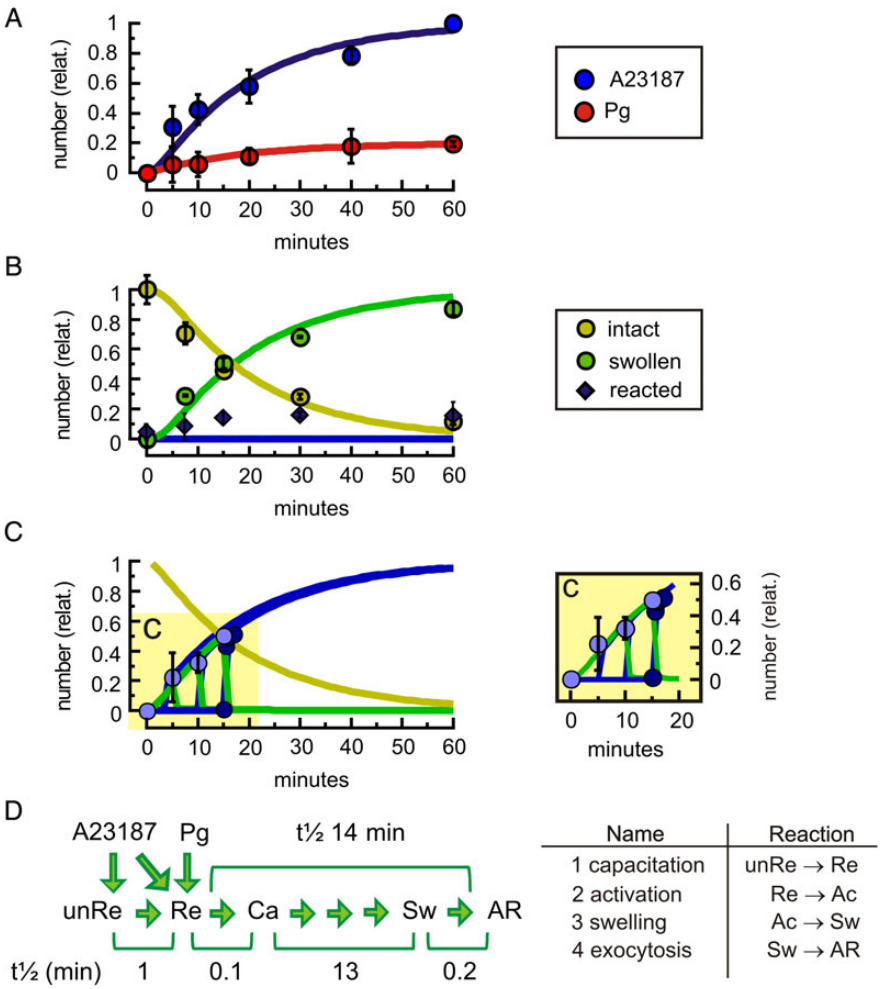

Figure 6 Kinetic model for the acrosome reaction. Acrosomal reaction was modeled in COPASI. The kinetic constants for 'activation' (entrance of calcium), 'swelling' (deformation of the acrosome) and 'exocytosis' (fusion pores opening and expansion) were calculated from experiments shown in Figs 2–4. The kinetics of 'capacitation' was estimated from results for mouse sperm reported in Tateno *et al.* (2013). (**A**) Proportion of reacted sperm as estimated by the model (blue line, calcium ionophore (A23157); red line, progesterone (Pg)) together with the corresponding experimental results from Fig. 2E. (**B**) Proportion of sperm with intact (yellow line), swollen (green line) or reacted (blue line) acrosomes as estimated by the model upon A23187 addition in the presence of an inhibitor of the Sw → AR reaction. The corresponding experimental results from Fig. 3A are also plotted. (**C**) Proportion of sperm with intact (yellow line), swollen (green line) or reacted (blue line) acrosomes as estimated by the model in the presence of a reversible inhibitor of the Sw → AR reaction. The inhibitor was inactivated 5, 10 or 15 min after A23187 addition. An enlarged version for the first minutes is shown at the right. The experimental results from Fig. 4C (blue circles) and 4D (gray circles) are also plotted. (**D**) A simplified scheme for acrosomal exocytosis including the estimated $t_{\frac{1}{2}}$ for all the reactions is shown on the left. The four reactions modeled in COPASI are shown on the right (unRe, unresponsive sperm; Re, responsive sperm; Ac, activated sperm; Sw, sperm with swollen acrosome; AR, reacted sperm).

1996; Henkel *et al.*, 1998; Rockwell and Storey, 2000; Caballero-Campo *et al.*, 2006; Harper *et al.*, 2006, 2008; Sanchez-Cardenas *et al.*, 2014). Although the dispersion of results is large, all studies reported values compatible with a slow kinetics that requires several minutes to hours to reach a plateau. Most studies showed that A23187 is a stronger inducer of the acrosome reaction that triggers exocytosis in a larger percentage of cells than other more physiological stimuli (e.g. progesterone or zona pellucida proteins). However, the reaction kinetics reported for different inducers requires several minutes to be completed. Our results indicate that acrosomal swelling in preparation for docking to the plasma membrane is a slow process that can strongly influence the velocity of the acrosome reaction. However, we are still far from understanding this process. The asynchrony in secretion indicates that the swelling, or a step within the swelling, is not completed at the same speed for all spermatozoa. In real-time experiments measuring simultaneously cytosolic calcium and the onset of acrosome reaction, it was reported that a calcium peak is observed just before exocytosis (Sanchez-Cardenas *et al*, 2014). This increase may be related to the release of calcium from intracellular stores that trigger the opening of fusion pores. A more detailed characterization of the swelling and its relationship with calcium signaling will be necessary to fully understand the kinetics of the acrosome reaction.

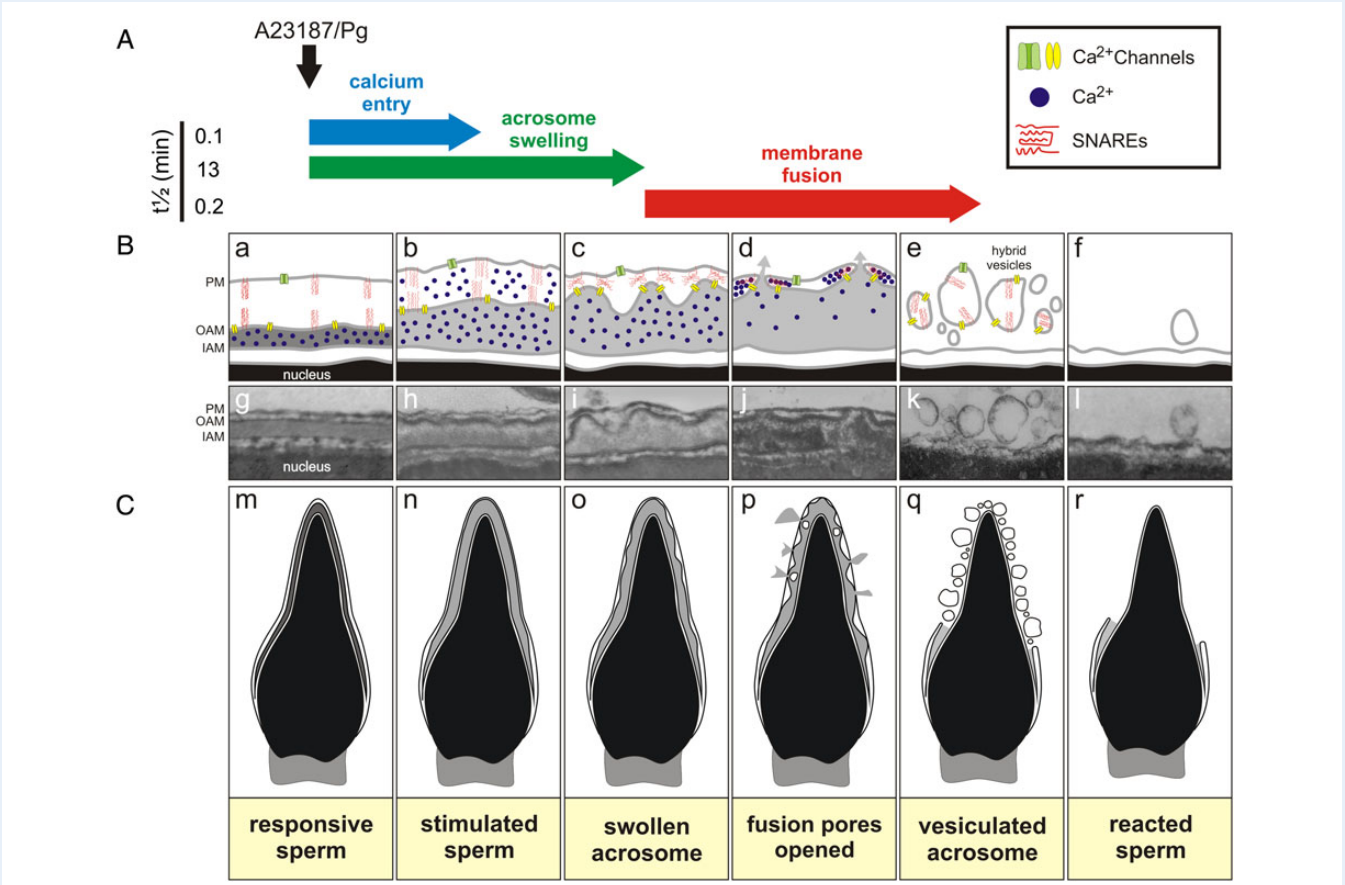

Figure 7 Kinetic model of the acrosome reaction. A summarizing model where the different steps studied in the present report are shown. Responsive (capacitated) spermatozoa undergo a fast increase in cytosolic calcium that triggers the swelling of the acrosome. Eventually, the outer acrosomal membrane is docked to the plasma membrane. The opening of calcium channels in the outer acrosomal membrane causes a local increase of this ion in the proximity of the membrane fusion machinery that triggers the opening of pores connecting the extracellular compartment with the acrosomal lumen. Expansion of these pores leads to acrosome vesiculation. The $t_{\frac{1}{2}}$ of these processes are shown in (**A**). The speculative changes in membrane topology including a few proteins that participate in the process are illustrated on the top part of (**B**). Selected electron micrographs representative of the proposed steps are shown in the lower part of this panel. (C) The corresponding morphological changes occurring in the sperm head during exocytosis.

Supplementary data

Supplementary data are available at http://molehr.oxfordjournals.org/online.

Acknowledgements

The authors thank Graciela Gutierrez, Alejandra Medero and Marcelo Furlán for excellent technical assistance and Claudia Tomes and Alberto Darszon for critically reading the manuscript.

Authors' roles

C.M.S., M.A.P., M.N.Z., F.C.M.Z. and G.A.D.B. contributed to the acquisition and analysis of data; and final approval of the version to be published. M.A.P., G.A.D.B. and L.S.M. designed the study, wrote the article and approved the version to be published. L.S.M. managed the project.

Funding

This work was supported by grants from Universidad Nacional de Cuyo, Argentina [06/J388 to L.S.M.]; Consejo Nacional de Investigaciones Científicas y Técnicas de Argentina [PIP 112-200801-02277 to L.S.M., PIP 114-201101-00409 to G.A.D.B.]; Agencia Nacional de Promoción Científica y Tecnológica de Argentina [PICT-2008-1114 to L.S.M., PICT-2011-2310 to L.S.M.], and fellowships from Consejo Nacional de Investigaciones Científicas y Técnicas de Argentina to C.M.S. and M.N.Z.

Conflict of interest

None declared.

References

Batiz LF, De Blas GA, Michaut MA, Ramirez AR, Rodriguez F, Ratto MH, Oliver C, Tomes CN, Rodriguez EM, Mayorga LS. Sperm from hyh mice

carrying a point mutation in alphaSNAP have a defect in acrosome reaction. *PLoS One* 2009;**4**:e4963.

Bello OD, Zanetti MN, Mayorga LS, Michaut MA. RIM, Munc13, and Rab3A interplay in acrosomal exocytosis. *Exp Cell Res* 2012;**318**:478–488.

Brewis IA, Clayton R, Barratt CL, Hornby DP, Moore HD. Recombinant human zona pellucida glycoprotein 3 induces calcium influx and acrosome reaction in human spermatozoa. *Mol Hum Reprod* 1996; **2**:583–589.

Caballero-Campo P, Chirinos M, Fan XJ, Gonzalez-Gonzalez ME, Galicia-Chavarria M, Larrea F, Gerton GL. Biological effects of recombinant human zona pellucida proteins on sperm function. *Biol Reprod* 2006;**74**:760–768.

Costello S, Michelangeli F, Nash K, Lefievre L, Morris J, Machado-Oliveira G, Barratt C, Kirkman-Brown J, Publicover S. Ca^{2+}-stores in sperm: their identities and functions. *Reproduction* 2009;**138**:425–437.

Darszon A, Nishigaki T, Beltran C, Trevino CL. Calcium channels in the development, maturation, and function of spermatozoa. *Physiol Rev* 2011;**91**:1305–1355.

De Blas G, Michaut M, Trevino CL, Tomes CN, Yunes R, Darszon A, Mayorga LS. The intraacrosomal calcium pool plays a direct role in acrosomal exocytosis. *J Biol Chem* 2002;**277**:49326–49331.

De Blas GA, Roggero CM, Tomes C, Mayorga LS. Dynamics of SNARE assembly and disassembly during sperm acrosomal exocytosis. *PLoS Biol* 2005;**3**:e323.

Harper CV, Kirkman-Brown JC, Barratt CL, Publicover SJ. Encoding of progesterone stimulus intensity by intracellular $[Ca^{2+}]$ ($[Ca^{2+}]$i) in human spermatozoa. *Biochem J* 2003;**372**:407–417.

Harper CV, Barratt CL, Publicover SJ, Kirkman-Brown JC. Kinetics of the progesterone-induced acrosome reaction and its relation to intracellular calcium responses in individual human spermatozoa. *Biol Reprod* 2006; **75**:933–939.

Harper CV, Cummerson JA, White MR, Publicover SJ, Johnson PM. Dynamic resolution of acrosomal exocytosis in human sperm. *J Cell Sci* 2008; **121**:2130–2135.

Henkel R, Franken DR, Habenicht UF. Zona pellucida as physiological trigger for the induction of acrosome reaction. *Andrologia* 1998;**30**:275–280.

Herrick SB, Schweissinger DL, Kim SW, Bayan KR, Mann S, Cardullo RA. The acrosomal vesicle of mouse sperm is a calcium store. *J Cell Physiol* 2005; **202**:663–671.

Hoops S, Sahle S, Gauges R, Lee C, Pahle J, Simus N, Singhal M, Xu L, Mendes P, Kummer U. COPASI—a COmplex PAthway SImulator. *Bioinformatics* 2006;**22**:3067–3074.

Hutt DM, Cardullo RA, Baltz JM, Ngsee JK. Synaptotagmin VIII is localized to the mouse sperm head and may function in acrosomal exocytosis. *Biol Reprod* 2002;**66**:50–56.

Hutt DM, Baltz JM, Ngsee JK. Synaptotagmin VI and VIII and syntaxin 2 are essential for the mouse sperm acrosome reaction. *J Biol Chem* 2005; **280**:20197–20203.

Inoue N, Ikawa M, Okabe M. The mechanism of sperm-egg interaction and the involvement of IZUMO1 in fusion. *Asian J Androl* 2011;**13**:81–87.

Jahn R, Fasshauer D. Molecular machines governing exocytosis of synaptic vesicles. *Nature* 2012;**490**:201–207.

Jimenez-Gonzalez C, Michelangeli F, Harper CV, Barratt CL, Publicover SJ. Calcium signalling in human spermatozoa: a specialized 'toolkit' of channels, transporters and stores. *Hum Reprod Update* 2006;**12**:253–267.

Lopez CI, Belmonte SA, De Blas GA, Mayorga LS. Membrane-permeant Rab3A triggers acrosomal exocytosis in living human sperm. *FASEB J* 2007;**21**:4121–4130.

Michaut M, Tomes CN, De BG, Yunes R, Mayorga LS. Calcium-triggered acrosomal exocytosis in human spermatozoa requires the coordinated activation of Rab3A and N-ethylmaleimide-sensitive factor. *Proc Natl Acad Sci USA* 2000;**97**:9996–10001.

Michaut M, De BG, Tomes CN, Yunes R, Fukuda M, Mayorga LS. Synaptotagmin VI participates in the acrosome reaction of human spermatozoa. *Dev Biol* 2001;**235**:521–529.

Ramalho-Santos J, Moreno RD, Sutovsky P, Chan AW, Hewitson L, Wessel GM, Simerly CR, Schatten G. SNAREs in mammalian sperm: possible implications for fertilization. *Dev Biol* 2000;**223**:54–69.

Rockwell PL, Storey BT. Kinetics of onset of mouse sperm acrosome reaction induced by solubilized zona pellucida: fluorimetric determination of loss of pH gradient between acrosomal lumen and medium monitored by dapoxyl (2-aminoethyl) sulfonamide and of intracellular Ca^{2+} changes monitored by fluo-3. *Mol Reprod Dev* 2000;**55**:335–349.

Rodriguez F, Zanetti MN, Mayorga LS, Tomes CN. Munc18-1 controls SNARE protein complex assembly during human sperm acrosomal exocytosis. *J Biol Chem* 2012;**287**:43825–43839.

Roggero CM, De Blas GA, Dai H, Tomes CN, Rizo J, Mayorga LS. Complexin/synaptotagmin interplay controls acrosomal exocytosis. *J Biol Chem* 2007;**282**:26335–26343.

Sanchez-Cardenas C, Servin-Vences MR, Jose O, Trevino CL, Hernandez-Cruz A, Darszon A. Acrosome reaction and Ca^{2+} imaging in single human spermatozoa: new regulatory roles of $[Ca^{2+}]_i$. *Biol Reprod* 2014;**91**:67.

Sudhof TC. Neurotransmitter release: the last millisecond in the life of a synaptic vesicle. *Neuron* 2013;**80**:675–690.

Tateno H, Krapf D, Hino T, Sanchez-Cardenas C, Darszon A, Yanagimachi R, Visconti PE. Ca^{2+} ionophore A23187 can make mouse spermatozoa capable of fertilizing *in vitro* without activation of cAMP-dependent phosphorylation pathways. *Proc Natl Acad Sci USA* 2013; **110**:18543–18548.

Tomes CN, Michaut M, De Blas G, Visconti P, Matti U, Mayorga LS. SNARE complex assembly is required for human sperm acrosome reaction. *Dev Biol* 2002;**243**:326–338.

Tomes CN, De Blas GA, Michaut MA, Farre EV, Cherhitin O, Visconti PE, Mayorga LS. alpha-SNAP and NSF are required in a priming step during the human sperm acrosome reaction. *Mol Hum Reprod* 2005; **11**:43–51.

Ward CR, Faundes D, Foster JA. The monomeric GTP binding protein, rab3a, is associated with the acrosome in mouse sperm. *Mol Reprod Dev* 1999;**53**:413–421.

Yanagimachi R. (1994). Mammalian fertilization. In Knobil E, Neill JD (eds). *The Physiology of Reproduction*. New York: Raven Press, 189–281.

Yunes R, Michaut M, Tomes C, Mayorga LS. Rab3A triggers the acrosome reaction in permeabilized human spermatozoa. *Biol Reprod* 2000; **62**:1084–1089.

Zanetti N, Mayorga LS. Acrosomal swelling and membrane docking are required for hybrid vesicle formation during the human sperm acrosome reaction. *Biol Reprod* 2009;**81**:396–405.

Zarelli VE, Ruete MC, Roggero CM, Mayorga LS, Tomes CN. PTP1B dephosphorylates N-ethylmaleimide-sensitive factor and elicits SNARE complex disassembly during human sperm exocytosis. *J Biol Chem* 2009; **284**:10491–10503.

Zoppino FC, Halon ND, Bustos MA, Pavarotti MA, Mayorga LS. Recording and sorting live human sperm undergoing acrosome reaction. *Fertil Steril* 2012;**97**:1309–1315.